Engineering Fracture Mechanics 76 (2009) 2698–2710

Contents lists available at ScienceDirect

Engineering Fracture Mechanics

journal homepage: www.elsevier.com/locate/engfracmech

An attempt to use scratch tests to predict the residual lifetime of unplasticised poly(vinyl chloride) pipes

H.A. Visser *, L.L. Warnet, R. Akkerman

Production Technology, Faculty of Engineering Technology, University of Twente, P.O. Box 217, 7500 AE, Enschede, The Netherlands

ARTICLE INFO

Article history:
Received 28 November 2008
Received in revised form 24 July 2009
Accepted 28 July 2009
Available online 3 August 2009

Keywords:
Polymers
Pipelines
Life prediction
Ductile-to-brittle transition
Toughness testing

ABSTRACT

This paper reports on a procedure that can potentially predict the residual lifetime of low-pressure uPVC pipes in a non-destructive way. Ageing of these materials is characterised by a change in yield stress and fracture behaviour. The search for a method being able to non-destructively evaluate the yield stress and the fracture behaviour led to the study of scratching of the polymer surface. According to an extensive study by Atkins and Liu, the scratching behaviour is a function of yield stress, fracture toughness and the attack angle of the cutting tool.

Experiments reported in this paper give an evaluation of the scratched area as a function of the attack angle for uPVC samples having different ageing times. Existing analyses for metals are adapted for polymer specific properties, such as the pronounced strain rate dependence of yield stress and visco-elastic recovery. The suggested adaptations are successful in the sense that the resulting analysis is capable of describing the forces during scratching and the resulting cross-sectional area of the groove. Although the scratching technique was not able to discriminate between differences in the scratch force or cross-sectional area of the groove of the different ageing times, it was possible to get an estimate of the fracture toughness from the analysis. Therefore, scratching is a promising technique to determine the fracture toughness for ductile materials for which it is difficult to obtain accurate results with conventional techniques.

1. Introduction

One of the oldest examples of the use unplasticised poly(vinyl chloride) (uPVC) in structural applications is its use in water and gas distribution systems. As for many structural applications, it is of great importance to have fundamental knowledge on how and when the polymer fails, not only for economical reasons, but mainly for risk analysis purposes. In the Netherlands, the first uPVC pipes used for the distribution of gas were installed in the early 1960s. These pipes were initially designed for a service life of 50 years. Although this limit is reached in the near future, failure registration data do not yet show any sign of a decrease in the integrity of the uPVC gas network [1]. As a consequence, the question has risen as to whether it is possible to extend the service life of the pipes. This has led to an increased interest for the development of a method to determine the condition and the residual lifetime of uPVC pipes. A non-destructive, in situ test method is preferred, as digging a pipe out of the ground for inspection is nearly as costly as replacement of the pipe.

Most failures in uPVC gas pipes occur due to incidents during excavation activities (third party damage). Therefore, it is of importance how an uPVC pipe fails upon impact loading. Ductile failure can not only absorb significantly more energy than

* Corresponding author. Tel.: +31 53 4894346; fax: +31 53 4894784.
E-mail address: h.a.visser@ctw.utwente.nl (H.A. Visser).

0013-7944/$ - see front matter © 2009 Elsevier Ltd. All rights reserved.
doi:10.1016/j.engfracmech.2009.07.021

Nomenclature

A_g	cross-sectional area of the groove underneath the original surface after (visco-) elastic recovery
A_{cut}	cross-sectional area of the groove underneath the original surface during cutting
A_{rub}	cross-sectional area of the groove underneath the original surface during rubbing
c	geometrical constant: the contact surface area between tool and specimen during scratching divided by the cross-sectional area of the groove
E	Young's modulus
F_f	horizontal force during scratching (parallel to specimen surface)
F_n	vertical force during scratching (perpendicular to specimen surface)
G_c	energy release rate
h_g	depth of groove underneath the original surface as measured after the scratch experiment.
H	indentation hardness
K_c	fracture toughness (critical stress intensity factor)
l_g	width of the groove at the original surface level
l_w	width of the groove between the ridges
Q	friction correction factor as defined by Eq. (3)
R	universal gas constant
R	crack resistance force
t	depth of groove underneath the original surface during scratching
T	temperature
ΔU	activation energy
v_{tip}	velocity of the tool tip with respect to the specimen
v^*	activation volume
Z	non dimensional parameter given by $R/(\tau_y t)$

Greek symbols

β	attack angle
β_{cr}	critical attack angle at which the transition between rubbing and cutting occurs
δ	tool tip half-angle (=26.6° for the tool used in this study)
$\dot{\varepsilon}$	strain rate
$\dot{\varepsilon}_o$	pre-exponential factor (determines thermodynamic state of polymer)
λ	friction angle
μ	friction coefficient in cutting conditions
μ'	friction coefficient in rubbing conditions
ν	Poisson's ratio
ϕ	shear plane angle
σ_y	tensile yield stress
τ_y	shear yield stress

brittle fracture, the gas flow out of the resulting leak is easier to stop as well. Therefore, ductile behaviour is preferred from a risk assessment point of view. The impact behaviour for glassy polymers, like uPVC, has a strong relation with the post-yield response of the material [2]. Both yield and post-yield behaviour can change over time due to physical ageing, which is a self retarding process during which the glassy polymer moves towards its equilibrium state, causing the physical and mechanical properties of the polymer to change [4–7]. Physical ageing increases the yield stress and strain softening (yield-drop), leading to more localised deformation [3] and thus embrittlement of a glassy polymer [2]. Following this statement, measurements of the plastic deformation behaviour can be used to determine the residual lifetime of uPVC gas pipes. It is a challenge, not to say almost impossible, to measure the yield behaviour of a material in a direct, non-destructive way. There are, however, techniques available that minimise the deformation during a measurement making the techniques non-destructive on a macroscopic scale. One promising technique to characterise the (physical) age by measuring the yield behaviour is micro-indentation [8]. Another promising technique is scratching. Recently, Atkins and Liu [9] presented an analysis that gives the opportunity to not only determine the yield behaviour, but also the fracture toughness using scratch measurements. The key is to change the attack angle of the tool and to observe at which angle the scratch behaviour changes from rubbing to cutting.

This paper aims to answer the question whether the analysis of Atkins and Liu can be applied to scratch measurements on uPVC pipes and to evaluate whether it is a promising technique to determine its residual lifetime in a "non"-destructive way. The analyses that are used were originally applied only to metals. Some adaptations are proposed to take polymer specific properties, such as the pronounced influence of strain rate on the yield stress and visco-elastic recovery, into account.

2. Theory

The authors do not intend to reproduce the current analysis on cutting and rubbing. A review has been proposed recently by Atkins and Liu [9] and more specifically on polymers by Briscoe and Sinha [10]. Only the important assumptions as made in [9] are summarised.

Besides the tool geometry, typical parameters that are varied during a scratch experiment are the scratch depth t or scratch force (F_n) and the attack angle of the tool β (see Fig. 1). The attack angle controls the transition between a cutting (high β) and a rubbing (low β) regime. A typical side view of a scratch experiment is shown in Fig. 1. In the cutting regime, the attack angle is such that material is removed. A shear plane angle φ exists, which is dependent on the attack angle, the friction angle on the tool rake face and the material used [11]. In the rubbing regime, material is simply displaced: a bow wave is formed in front of the tool tip, which is pushed to the side of the groove, eventually resulting in a shape with a cross-section as shown schematically in Fig. 2.

The transition between rubbing and cutting has originally been described by Sedriks and Mulhearn [12,13]. Their approach also showed good agreement between the change in cross-sectional area of the groove (A_g, see Fig. 2) and the attack angle for dead-weight loading measurements on lead and copper.

An expression for the cross-sectional area of the groove in the rubbing regime is derived from an approach by Bowden and Tabor [14], who divided the sliding force into a shearing and a ploughing component:

$$A_{rub} = \frac{\mu' F_n}{c(H + \tau_y \cot\beta)}, \tag{1}$$

where F_n is the normal force, τ_y the shear yield stress, H the dynamic scratch hardness, or hydrostatic pressure yield stress (equal to the force during scratching divided by the area of the contact surface), μ' the coefficient of friction in rubbing conditions and c a geometrical constant (the ratio between the actual area of contact between the material and the face of the tool and the cross-sectional area of the groove during scratching), which corrects for pile up during scratching.

In the cutting regime, the ploughing term in Bowden and Tabor's analysis is rearranged using a force equilibrium similar to that of Merchant [15] to give an expression for the cross-sectional area of the groove during cutting:

$$A_{cut} = \frac{F_n[1 + \mu\tan(\beta - 90^\circ)]}{cH[\mu - \tan(\beta - 90^\circ)]}. \tag{2}$$

Still, some simplifying assumptions gave the opportunity for other authors to re-examine the analysis of Sedriks and Mulhearn. Especially in the cutting regime, Atkins and Liu [9] have shown that not only plasticity and friction should be taken into account, but also the surface work necessary to create the chip. This led to expressions for the normalised friction force ($F_f/(\tau_y t^2)$, with F_f the horizontal force, τ_y the shear yield stress and t the depth of the tool during scratching) in both regimes as a function of the attack angle. For the rubbing regime Atkins and Liu adopted the upper boundary model under high friction conditions as described in the appendix of [16]. At cutting conditions, it is shown that this sliding force depends on a value $Z = R/\tau_y t$, where R is the crack resistance force, according to:

$$\frac{F_f}{\tau_y t^2} = \frac{1}{Q}\left(\frac{\tan\delta}{\cos(\beta - 90^\circ - \phi)\sin\phi} + \frac{2Z}{\cos\delta}\right). \tag{3}$$

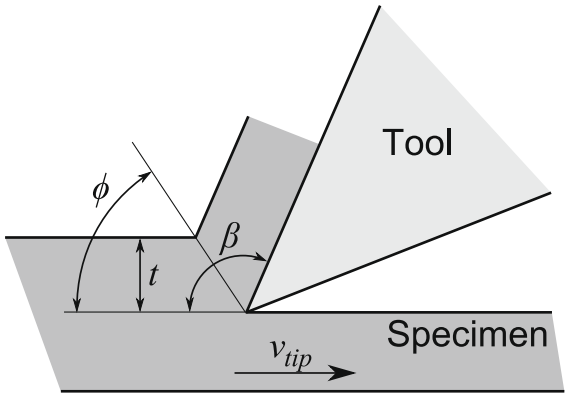

Fig. 1. Definition of the attack angle (β), the shear plane angle (ϕ), the scratch depth (t) and the speed of the tool tip with respect to the specimen (v_{tip}) during scratching.

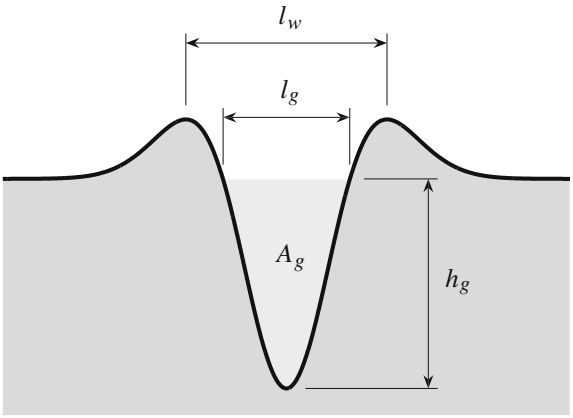

Fig. 2. Geometry of a resulting groove, including the definition of the width of the groove between the ridges (l_w) the width of the groove at the original surface level (l_g), cross-sectional area of the groove (A_g) and the depth of the resulting groove (h_g).

With:

$$Q = 1 - \frac{\sin\lambda \sin\phi}{\cos(\lambda - \beta + 90^\circ)\cos(\beta - 90^\circ - \phi)}. \tag{4}$$

This analysis gives an explanation for the material dependency of the shear plane angle (ϕ, see Fig. 1), the friction angle (λ), as well as providing a potential method for measuring fracture toughness values of tough materials that are difficult to measure by other methods.

3. Experimental

3.1. Materials

All specimens used for this research were taken out of a new, unused Ø110 mm uPVC pipe that was originally produced for water distribution purposes. Sections of 70 mm were cut with a bandsaw from the pipe material and subsequently sawed in axial direction. These parts were then pressed into flat plates in a press at 100 °C. Subsequently, the plates are cooled down to room temperature within two minutes in a cold press. Tensile bars with a parallel gauge section of approximately $30 \times 5 \times 3$ mm^3 were milled from the plate material. The plates that were used for scratching were cut with a bandsaw to the dimension of $69 \times 69 \times 3$ mm^3. The specimens were divided over four samples, which received different heat treatments. One sample received no heat treatment and will be referred to as the *as-manufactured* sample. Three samples were aged at 60 °C in a convection oven for $1{\cdot}10^4$ s, $1{\cdot}10^5$ s and $1{\cdot}10^6$ s. Since the process of physical ageing is accelerated at increased temperatures [17,18], the heat treatments will lead to a change in the thermodynamic state and hence the mechanical properties of the specimens. The sample that received the longest heat treatment is referred to as *aged*.

3.2. Test method

The tensile tests to determine the yield stress of the specimen were carried out on a MTS Elastomer Testing System 810 equipped with a 25 kN force cell and a temperature controlled chamber. The yield stress was measured at temperatures ranging from −20 °C to 40 °C. The specimens were allowed to reach the test temperature by installing the specimen at least 10 min prior to testing. The tensile tests were carried out at constant engineering strain rates ranging from 10^{-5} s^{-1} up to 1 s^{-1}. The (engineering) yield stress was measured from the force at yielding and the initial cross-sectional area of the specimen (an average of three measurements along the gauge section of the specimen).

The scratch experiments were carried out on a custom built setup, which is shown in Fig. 3. The setup consists of a moving head, in which the tool is mounted, and a moving table upon which the specimen is mounted. The head can move in the *z*-direction and is equipped with two force cells, measuring the forces in both the *z*- and *x*-direction. The construction of the force cells is such that, in essence, the situation is similar to the schematic representation shown in Fig. 3, with the vertical force cell attached to the head and the horizontal force cell to the moving table. The movement of the head is force controlled. Consequently, only deadweight scratch tests can be carried out on the setup. The table on which the specimen is mounted can move in both the *x*- and *y*-direction using two PI M-505.2 PD micropositioning stages. The tool is mounted in a Thorlabs RSP05/M rotational stage that allows changes in the attack angle. The tool geometry as shown in Fig. 4 was machined by electro-erosion.

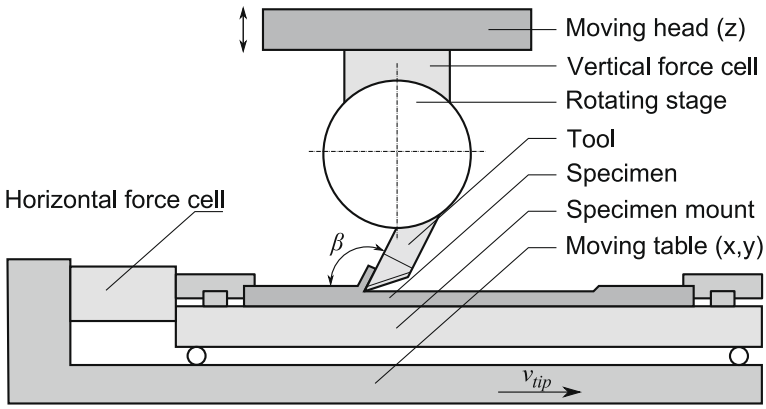

Fig. 3. Schematic representation of the experimental setup as used for the scratch experiments.

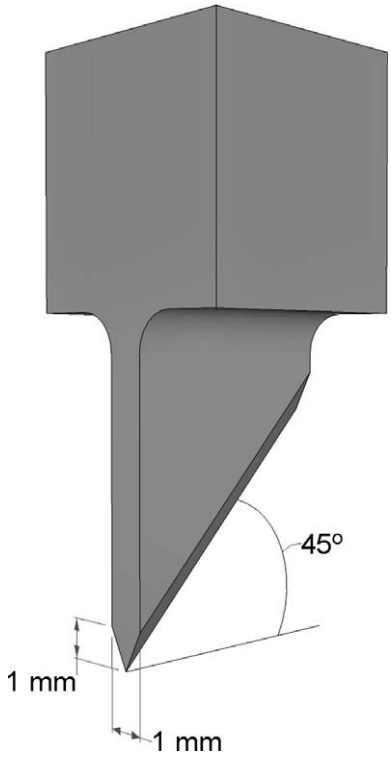

Fig. 4. Geometry of the tool used for the scratch experiments.

Each measurement consisted of three scratches with a length of 15 mm. All measurements were carried out with a horizontal scratch velocity (v_{tip}) of 1 mm/s and a vertical force (F_n) of 1 N.

The geometry of the groove was measured for some of the measurements using a white light interferometer (Atos Micromap 560). The time between scratching and measuring the groove geometry was at least three hours, so no significant changes of the groove geometry are to expect during the measurement due to visco-elastic recovery [20].

4. Results

4.1. Measured forces

Both the normal as well as the horizontal force have been logged during the scratch measurements. A typical result of the force versus the scratch length is shown in Fig. 5. The vertical force initially grows after which the force is controlled to 1 N

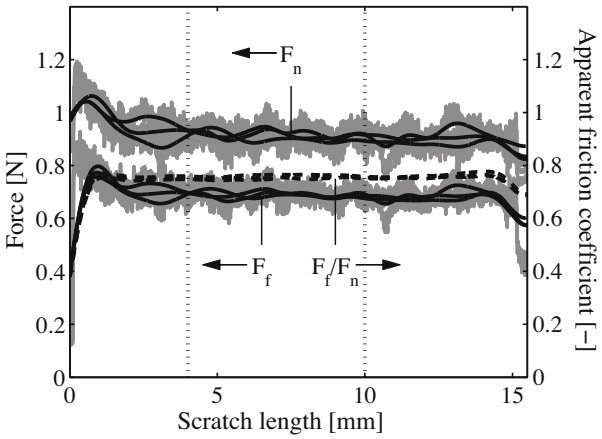

Fig. 5. Unfiltered force signals (grey), filtered force signals (black) and filtered apparent friction coefficient (dashed) for three scratches at an attack angle of 40° on an as-manufactured specimen.

again. The amplitude of the noise on the signal is about 0.1 N for all force measurements. This noise is filtered out using a second order lowpass digital Butterworth filter (solid lines in Fig. 5). From the filtered signal it can be concluded that the normal force is not exactly controlled at 1 N. This is possibly caused by surface defects on the specimen. The normal forces for all three scratches show similar behaviour.

The horizontal force (F_f) follows the same behaviour as the normal force, but it is shifted towards lower forces for this specific attack angle (the level of F_f depends on β). The horizontal force is not only a resultant of frictional forces, but also of plasticity and, in the case of cutting, of the surface work energy contribution to F_f. Therefore, the ratio between the horizontal force and the vertical force will be referred to as the "*apparent* friction coefficient" throughout this paper. The apparent friction coefficient proves to be nearly constant for most of the scratch length and for most of the attack angles, including the measurement at 40° as depicted in Fig. 5.

Only a part of the force signals were taken into account in the further analysis. The unstable start of the scratch was omitted and the signal was evaluated between 4 and 10 mm of scratch length. The results are not sensitive to the choice of the latter limit as long as it is below 15 mm and therefore this choice is rather arbitrary.

The reproducibility of the measurement of the apparent friction coefficient is good as shown in Fig. 6. A clear trend of increasing apparent friction coefficient with increasing attack angle is visible. Three regimes are observed during the measurements with an increasing attack angle. Firstly, no chip is formed at attack angles up to about 60° and only ploughing or rubbing occurs. The angle at which this transition occurs is defined as the critical attack angle (β_{cr}). Secondly, discontinuous chips are formed for attack angles between about 60° and 70°. The formation of discontinuous chips results in the occurrence of a crackling noise during scratching. The rise and fall of the horizontal force related to the build up and fracture of a small chip results in some variation in the apparent friction coefficient, as shown in Fig. 6 for the case of an attack angle of 65°. Finally, continuous chips are formed at attack angles larger than about 70°. The force signals for scratches with continuous chip formation are more constant. As the attack angle increases, the chances of seizure (i.e. the tool digging in) increases. Therefore, no force controlled measurements can be conducted at attack angles greater than 90°.

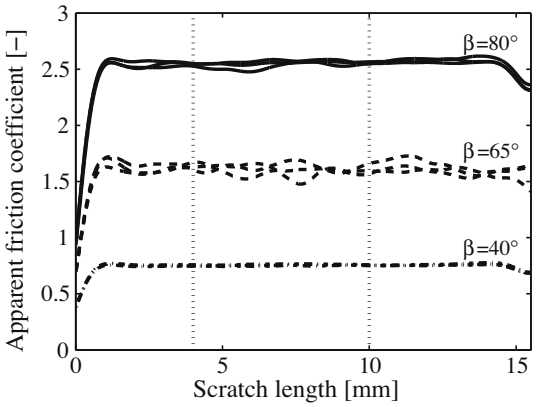

Fig. 6. Filtered apparent friction coefficients during scratching for three different attack angles on an as-manufactured specimen.

The average apparent friction coefficient (over the selected part of the scratch) is plotted against the attack angle for specimens that received different heat treatments in Fig. 7. Each data point is the average of three measurements. The standard deviation is indicated by error bars, but as the standard deviation is very low, most error bars are covered by markers. The three previously mentioned regions are also observed in the force signal. Around 60° the apparent friction coefficient has a sudden steep rise. At larger attack angles the coefficient becomes almost independent of the attack angle, up to about 70°, where the coefficient increases again with the attack angle until seizure occurs.

The tensile yield stress of the uPVC specimens was measured at room temperature and at an arbitrarily chosen engineering strain rate of 10^{-3} s^{-1} to quantify the influence of the heat treatments on the yield behaviour. For the as-manufactured sample an engineering yield stress of 50.1 MPa was measured. For the aged samples 51.9 MPa, 53.6 MPa and 55.0 MPa was found (in order of increasing aging time). As expected, the yield stress increases with physical ageing. Therefore, it is expected that the amount of deformation during scratching at a constant normal force will decrease. This should cause a decrease in the horizontal force during ploughing and thus an increase in the critical attack angle., The experimental data in Fig. 7 shows, however, neither consistent nor significant differences between the four samples that received different heat treatments. Apparently, the scratch force is scarcely influenced by the increase in yield stress. To investigate whether the scratch itself is influenced by physical ageing, the geometry of the resulting groove was measured.

5. Geometry of the resulting groove

The geometry of the groove was measured approximately three hours after the scratch experiment using interference microscopy. The interference patterns were only obtained for the surfaces that were more or less perpendicular to the light beam of the microscope. Therefore, little data was obtained for the slopes of the grooves as can be seen in Fig. 8, where three typical measurements of grooves from each of the three previously mentioned regimes are shown. For each attack angle only one groove (the second of the three) was measured at approximately half of the scratch length. Each measurement scans a

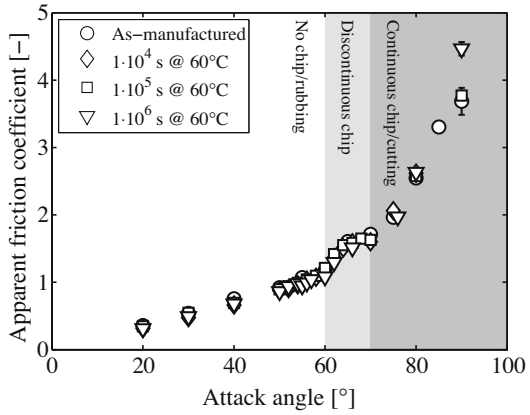

Fig. 7. Apparent friction coefficient versus attack angle for uPVC specimens that were aged for different ageing times at 60 °C.

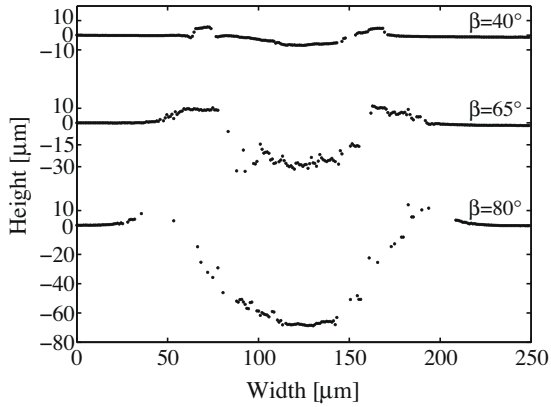

Fig. 8. The measured groove size for three scratches at different attack angles on an as-manufactured specimen.

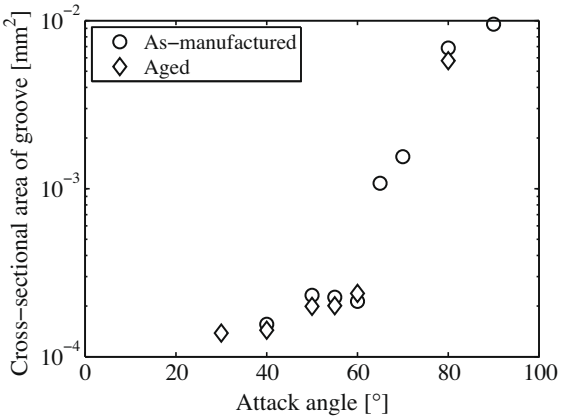

Fig. 9. The cross-sectional area of the groove (A_g) versus the attack angle (β) for a as-manufactured and aged ($1 \cdot 10^6$ s at 60 °C) uPVC specimens.

groove length of 0.3 mm. The resulting cross-sectional area of the groove (A_g) is plotted on a logarithmic scale versus the attack angle in Fig. 9. Within the attack angle range where no chip is formed (up to 60°) the cross-sectional area of the groove increases slightly with the attack angle. At the moment when chips are formed, the cross-sectional area of the groove increases steeply with the attack angle. Again, no consistent differences are found between the grooves on the as-manufactured and the aged specimens. The differences that are present can only be attributed to scatter in the measurements; no significant differences for both the force signals and the groove geometry have been found between the as-manufactured and the aged specimens. The different models that were presented in the Theory section have been elaborated with these data, to explore whether these models support the experimentally obtained result.

6. Discussion

6.1. The influence of physical ageing according to the theory

Firstly, the theory of Sedriks and Mulhearn presented in [12,13] will be applied on the data, to find out whether a significant shift of the critical attack angle as a result of physical ageing is expected from theory. The model is summarised in Eqs. (1) and (2). Sedriks and Mulhearn found that for scratch measurements on lead the value of c ranged between 1.5 and 2.5 for different attack angles [12]. According to Atkins and Liu [9] the value of c depends on the half-angle of the tool tip; it increases with a decreasing angle. In this study the tool has a smaller tool tip half-angle than the one used by Sedriks and Mulhearn (27° as opposed to 45°). As a first approximation the maximum value of the range found by Sedriks and Mulhearn ($c = 2.5$) will be used throughout this study. Additional measurements are required to verify this approximation. The values for the coefficients of friction μ and μ' are assumed to be equal and related to the critical attack angle (β_{cr}) as follows [13]:

$$\tan(90^\circ - \beta_{cr}) = \frac{1-\mu^2}{2\mu}. \tag{5}$$

With $\beta_{cr} = 60^\circ$ a value of $\mu = 0.58$ was found.

Before applying the model of Sedriks and Mulhearn to a glassy polymer instead of a metal (for which it was originally proposed), two polymer specific properties should be taken into account. Firstly, the strain rate and temperature dependence of the (shear) yield stress (as shown in Fig. 10 for uPVC) is much more pronounced for glassy polymers than for metals. Therefore, the values of the shear yield stress (τ_y) and the dynamic hardness (H) in equation (1) and (2) depend on the strain rate encountered during scratching. Secondly, glassy polymers are visco-elastic materials. Consequently, the groove resulting from the scratch experiment, (partly) recovers in time. Therefore, post-mortem measurements of the groove cannot be directly used to calculate the contact surface area during scratching. In the next section both these effects will be incorporated in the model of Sedriks and Mulhearn.

The yield stress of glassy polymers is more sensitive for the deformation rate and temperature than that of metals. The strain rate dependence should be taken into account to obtain the correct value for the yield stress of the polymer material around the tool tip. The exact strain field of the material below the tool tip during scratching is very complex, and can only be calculated using a finite element approach and the intrinsic deformation behaviour of the material such as done in [19] for rubbing conditions. Here, an estimation proposed by Gauthier and Schirrer [20] for the strain rate in the far field from the tip has been used:

$$\dot{\varepsilon} = \frac{v_{tip}}{l_w}, \tag{6}$$

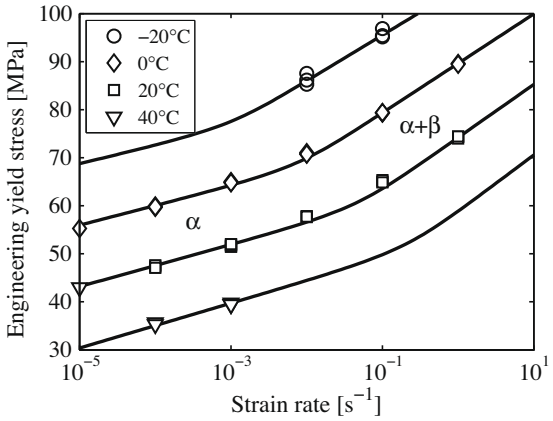

Fig. 10. Engineering tensile yield stress versus engineering strain rate of uPVC as measured at various temperatures. The solid lines show the results of employing the Ree-Eyring expression in Eq. (7) with the parameters given in Table 1.

with v_{tip} the speed of the tool tip (1 mm/s in this case) and l_w the width of the groove between the ridges (see Fig. 2) which is measured to be about 100 μm on average (see Fig. 8), resulting in strain rates of approximately 10 s^{-1}. This strain rate is four orders of magnitude higher than the applied tensile strain rate in the tensile tests presented earlier. Nevertheless, the yield stress of the material around the tool tip (thus at a strain rate of 10 s^{-1}) for each sample can be calculated from the yield stress measurements at 10^{-3} s^{-1} by characterising the deformation kinetics of uPVC. The strain rate and temperature dependence of the yield stress of uPVC as measured with uniaxial tensile test is shown with markers in Fig. 10. In the low temperatures and high strain rate region clear transitions in the yield behaviour can be observed. This thermorheologically complex behaviour can be attributed to two relaxation processes: the α- and the β-transition. The α-transition is related to main chain segmental motion, whereas the β-transition is related to side-chain mobility. Since the work of Roetling (for example [21]), thermorheological complex yield behaviour of polymers is commonly described with a Ree-Eyring expression [22]:

$$\frac{\sigma}{T} = \sum_{x=\alpha,\beta} \frac{R}{v_x^*} \sinh^{-1}\left[\frac{\dot{\varepsilon}}{\dot{\varepsilon}_{0,x} \exp\left(-\frac{\Delta U_x}{RT}\right)}\right], \tag{7}$$

where R is the universal gas constant, v^* the activation volume, ΔU the activation energy and $\dot{\varepsilon}_0$ a pre-exponential factor that depends on the thermodynamic state of the material and is thus different for each sample. This pre-exponential factor(s) can be calculated from a reference yield stress. For the activation volume a value of $1.29 \cdot 10^{-3}$ m^3/mol for the α-process and $8.39 \cdot 10^{-4}$ m^3/mol for the β-process was found. The activation energy values are 297 kJ/mol and 59 kJ/mol, respectively. These values are similar to the values reported by Bauwens-Crowet et al. [23] for uPVC and summarised in Table 1. The resulting model description is shown as solid lines in Fig. 10, which accurately follow the experimentally observed yield behaviour. With the measured tensile yield stress at 10^{-3} s^{-1}, $\dot{\varepsilon}_0$ of each sample can be calculated, which is used to calculate the yield stress at 10 s^{-1}. For polymers, the shear yield stress (τ_y), as used by Sedriks and Mulhearn in Eq. (1), is equal to the tensile yield stress (σ_y) divided by $\sqrt{3}$, resulting in values of 48.0 MPa for the as-manufactured sample and 50.8 MPa for the aged sample.

Table 1
Summary of the material parameters used in this paper for uPVC. For the parameters that are influenced by the thermodynamic state the value for both the as-manufactured and the aged specimens is given. The parameters for which no source is given were determined using experimental data presented in this paper.

Parameter	As-manu-factured	Aged	Units	Source
μ	0.58		(–)	
v_α^*	$1.29 \cdot 10^{-3}$		(m^3/mol)	
v_β^*	$8.39 \cdot 10^{-4}$		(m^3/mol)	
ΔU_α	297		(kJ/mol)	
ΔU_β	59		(kJ/mol)	
$\dot{\varepsilon}_{0,\alpha}$	$1.73 \cdot 10^{38}$	$1.34 \cdot 10^{37}$	(s^{-1})	
$\dot{\varepsilon}_{0,\beta}$	$2.33 \cdot 10^{9}$		(s^{-1})	
τ_y (at 10 s^{-1})	48.0	50.8	(MPa)	
H (at 10 s^{-1})	168	178	(MPa)	$=2 \cdot \sigma_y$ [20]
E	3		(GPa)	[25]
ν	0.38		(–)	[25]

The dynamic hardness (H) is another material property in the model of Sedriks and Mulhearn that depends on the strain rate and temperature for glassy polymers. Gauthier and Schirrer [20] showed that the strain rate and temperature dependence of the dynamic hardness of poly(methylmethacrylate) (PMMA) could be described with a relation similar to Eq. (7), using parameter values that agree well with those usually obtained for the tensile yield stress of PMMA. Therefore, a linear dependence can be expected between the dynamic hardness and the yield stress at a certain strain rate and temperature. Here, the approximation that the dynamic hardness is approximately twice the yield stress [20] was used, leading to values of 168 MPa for the as-manufactured sample and 178 MPa for the aged sample.

Sedriks and Mulhearn use the cross-sectional area of the groove (A_g) to calculate the contact area between the tool and the specimen during scratching (assuming $t = h_g$). The factor c is used to correct for pile up during scratching. The relation between the cross-sectional area of the groove (A_g) and the contact area between tool and specimen is less obvious for polymers. Due to a lower Young's modulus for uPVC than for metals (approximately one order of magnitude lower) and the visco-elastic behaviour of polymers the cross-sectional area of the groove during scratching is not identical to the cross-sectional area of the groove as measured after scratching. The depth/width ratio of the groove during scratching ($=t/l_g$) should be identical to the vertical projection of the tool tip. The vertical projection is equal to the front view of the tool, which is shown on the right side of Fig. 11 for two attack angles. This vertical projection, and thus the ratio, changes with the attack angle according to:

$$\frac{t}{l_g} = \frac{\sin\beta}{2\tan\delta}, \tag{8}$$

where t is the depth of the groove during scratching (actual depth) and δ the tool tip half-angle. Both the actual depth/width ratio during scratching and the measured ratios after visco-elastic recovery ($=h_g/l_g$) are plotted in Fig. 12. The relaxation of the groove depth due to the visco-elastic effect is more distinct than that of the groove width. This results in a lower depth/width ratio after visco-elastic recovery, when compared to the theoretical prediction using Eq. (8). Therefore, the influence of

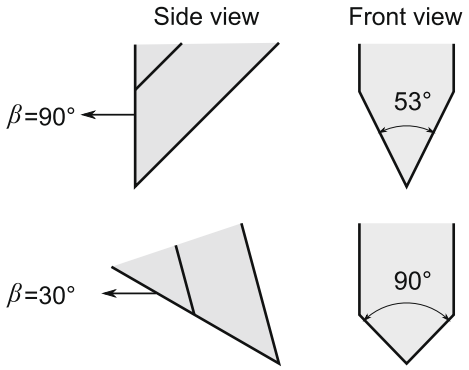

Fig. 11. Side and front view of the tool for two attack angles (β). For an attack angle of 90° the angle of the tip as viewed from the front is equal to the actual tool tip angle (53°). For an attack angle of 30°, the angle of the tool tip as viewed from the front is 90°.

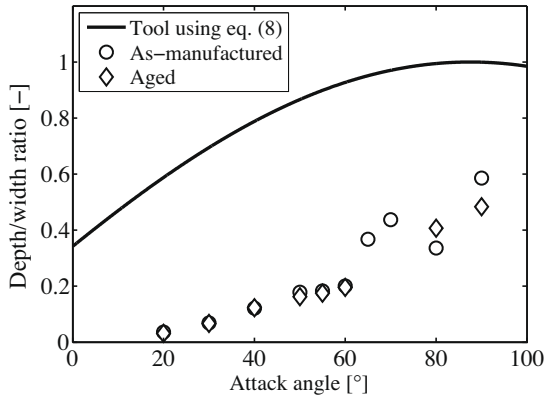

Fig. 12. Comparison between the theoretical depth/width ratio for the tool (t/l_g using Eq. (8)) and the depth/width ration as measured (h_g/l_g) for as-manufactured and aged ($1 \cdot 10^6$ s at 60 °C) uPVC specimens at a range of attack angles (β).

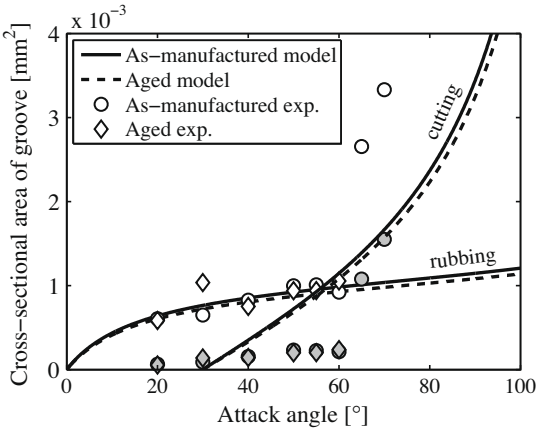

Fig. 13. Comparison between measurements and the model as proposed by Sedriks and Mulhearn given by Eqs. (1) and (2). The markers filled in grey represent the data that are not corrected for (visco-)elastic recovery, whereas the white filled markers are the corrected values.

the visco-elastic recovery should be taken into account when the cross-sectional area of the groove is used to calculate the actual contact area between the tool and the material during scratching, as is done in the model of Sedriks and Mulhearn [12]. In this study the influence of the visco-elastic recovery on the width of the groove (l_g, see Fig. 2) is neglected and thus visco-elastic recovery is assumed to influence only the depth of the groove. The measured groove width was used to calculate t according to Eq. (8), from which the cross-sectional area of the groove during scratching was calculated. The resulting value is referred to as the *corrected* cross-sectional area of the groove throughout the rest of this paper.

With the assumptions for obtaining the yield stress, the hardness and the corrected cross-sectional area of the groove, the model results can be compared with the results of measurements. Both the raw data (gray filled markers) as the corrected data (white filled markers) of the measurements are shown in Fig. 13. The measurements at the attack angles 80° and 90° are not shown as the corresponding cross-sectional area of the grooves were greater than $4 \cdot 10^{-3}$ mm^3. The model for the rubbing mechanism describes the corrected measurements very well, whereas the model for the cutting regime describes the raw data better. The visco-elastic recovery is apparently larger for a groove created by rubbing, than for a groove created by cutting, which complies with the fact that during cutting material is removed and thus recovery of the groove is limited. Following this reasoning the corrected cross-sectional area of the groove should, however, be almost equal to the measured cross-sectional area of the groove, which is not the case. Apparently, the groove width (l_g) as measured post-mortem is not equal to the groove width during scratching, which might be related to the fracture behaviour during cutting. Additional measurements are required to confirm this explanation.

Another conclusion that can be drawn from Fig. 13 is that the model supports the experimental observations on the differences between the as-manufactured sample and the aged sample. The model predicts only minor differences between the as-manufactured sample and the aged sample. Apparently, the cross-sectional area of the groove is hardly influenced by a change in the yield stress. The proposed measurement technique in its current form can therefore not be used to measure the residual lifetime of the uPVC pipe material. To find out whether it is possible to determine the fracture toughness of the material, the already presented analysis of Atkins and Liu that includes the surface work, was applied on the measured data. The results are presented in the next section.

7. Determining the fracture toughness by scratch measurements

The mode I fracture toughness (K_{Ic}) is a difficult property to measure for ductile materials such as uPVC, as macroscopic plastic deformation occurs prior to crack growth failure, making the experiments either invalid or complicate the analysis. Consequently, there is a large scatter on the data reported in literature. In e.g. [26,27] values between 2.5–6.5 MPa m^{½} are reported for the fracture toughness of uPVC. In their analysis of scratch measurements at different attack angles Atkins and Liu [9] showed that the critical attack angle (β_{cr}) is related to the fracture toughness of a material. In this section the presented experimental scratch data on uPVC are used to verify whether the scratch test is a promising alternative procedure to deduct the fracture toughness of ductile materials.

In the analysis including surface work as proposed by Atkins and Liu [9] the normalised force is plotted against the attack angle (shown in Fig. 14). The normalised rubbing force remains nearly constant for the corrected measurement data. When the cutting regime is entered the normalised force suddenly drops due to the steep increase in the cross-sectional area of the groove (as already shown in Figs. 9 and 13). The results for the upper bound model under high friction conditions for a tool tip half-angle (=26.6° in this study) is obtained in a similar way as described in the appendix of [16]. The surface work model (Eqs. (3) and (4)) was fitted to the experimental data using Z and ϕ as fit parameters. Atkins and Liu [9] proposed the following relation for the friction angle λ:

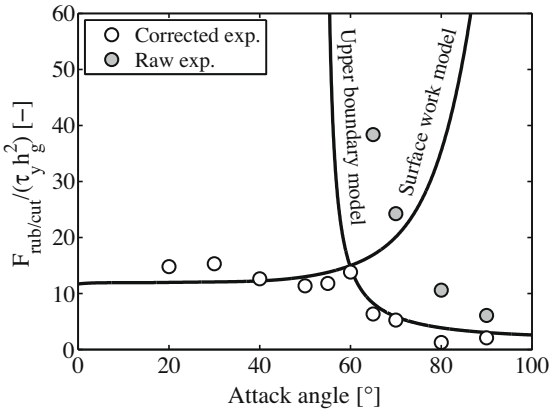

Fig. 14. The normalised rubbing and cutting force versus the attack angle for both corrected (white filled markers) and raw (grey filled markers) experimental data. The lines represent the results for the analysis as proposed by Atkins and Liu [9].

$$\lambda = \arctan\left(\frac{F_f}{F_n}\right) + \beta - 90^\circ. \tag{9}$$

Here, a linear relation was found between λ and β in the experimental data ($\lambda = 0.148 \cdot \beta$), which was employed calculate the value for λ as used in the Eqs. (3) and (4). With this approximation the fit resulted in a value of 0.1 for Z and a shear plane angle of 46°, which is in line with the observations reported in the pioneering work of Kobayashi [24]. The result of the upper boundary model is shown as a solid line and the result of the surface work model (using Eqs. (3) and (4)) is shown as a dashed line in Fig. 14. From Z and the previously obtained value for the shear yield stress, the crack resistance force R can be calculated at the critical attack angle (=60°). Neglecting both the kinetic and dissipative energy in the Griffith energy balance ($R = G_c$) and assuming plane strain conditions during cutting; the fracture toughness or critical stress intensity factor (K_c) can be calculated with:

$$K_c = \sqrt{\frac{ER}{1-\nu^2}}. \tag{10}$$

Although the Young's modulus is known to also depend on the thermodynamic state for uPVC [5], a standard textbook value will be used here. For the Young's modulus (E) and the Poisson's ratio (ν) values of 3 GPa and 0.38 [25] are used, respectively, resulting in $K_c \approx 0.7$ MPa $m^{1/2}$. The analysis provides a K_c that is in the correct order of magnitude, but lower, when compared to values reported in literature. Due to a sum of approximations in the analysis it is, at this stage, difficult to exactly put forward an explanation for the low value. Another point worth mentioning is that the K_c value found with this scratching analysis does not necessarily relate to pure mode I deformation, as discussed in [28]. Therefore, the K_c value found with the scratch analysis might be expected to be too high than too low.

8. Conclusions

A custom built apparatus was presented on which it is possible to perform force controlled scratch measurements at different attack angles. Three regimes are observed for uPVC: ploughing (no chip formation) at low attack angles, cutting (continuous chip formation) at high attack angles and an intermediate region (discontinuous chip formation) at attack angles between 60° and 70°. In the cutting region the horizontal force increases rapidly with increasing attack angles, up to about 90° where seizure occurs and thus no force controlled measurements can be conducted. The influence of the attack angle on both the horizontal force and the cross-sectional area of the groove was measured for samples that received different ageing treatments. No significant difference in the scratch behaviour of the samples was observed, despite the distinct difference in yield stress.

The analysis of Sedriks and Mulhearn was applied on the uPVC scratch data. Two effects typical for glassy polymers were taken into account: the strain rate and temperature dependency of the yield stress and visco-elastic recovery of the groove. After compensating the depth of the groove, the analysis gives a good description of the measurement data. The analysis for the aged sample only gives minor differences compared to that of the as-manufactured one, confirming the experimental observations. Therefore, the main conclusion that can be drawn is that the current setup is not capable of measuring the residual lifetime of the uPVC pipe material. Nevertheless, the analysis including the surface work during cutting makes it possible to make an estimation of the fracture toughness of the material. The scratching technique presented in this paper might, therefore, be a promising method to characterise the toughness of ductile materials for which it is difficult to use conventional techniques.

Acknowledgements

The financial support of the four gas network operators Cogas Infra & Beheer BV, Enexis, Liander and Stedin is gratefully acknowledged by the authors. Furthermore, gratitude goes out to G. van der Linde of the Laboratory for Surface Technology and Tribology at the University of Twente and the Polymer Technology group at Eindhoven University of Technology for their support on the experimental work.

References

[1] Hermkens RJM, Wolters M, Weller J, Visser HA. PVC pipes in gas distribution: still going strong! Budapest: proceedings of plastic pipes, vol. XIV; 2008.
[2] Melick HGH, van Govaert LE, Meijer HEH. Localisation phenomena in glassy polymers: influence of thermal and mechanical history. Polymer 2003;44(12):3579–91.
[3] Cross A, Haward R, Mills N. Post yield phenomena in tensile tests on poly(vinyl chloride). Polymer 1979;20(3):288–94.
[4] Struik LCE. Physical aging in amorphous polymers and other materials. Amsterdam: Elsevier; 1978.
[5] Hutchinson JM. Physical aging of polymers. Prog Polym Sci 1995;20(4):703–60.
[6] Ott HJ. Einfluß der thermischen Vorgeschichte auf die mechanischen Eigenschaften von amorphen Thermoplasten. Colloid Polym Sci 1980;258(9):995–1008.
[7] Rabinovitch EM, Summers JW. The effect of physical aging on properties of rigid polyvinyl chloride. J Vinyl Technol 1992;14(3):126–30.
[8] Breemen LCA, van Engels TAP, Pelletier CGN, Govaert LE, den Toonder JMJ. Numerical simulation of flat-tip micro-indentation of glassy polymers: influence of loading speed and thermodynamic state. Phil Mag 2009;89(8):677–96.
[9] Atkins AG, Liu JH. Toughness and the transition between cutting and rubbing in abrasive contacts. Wear 2007;262(1–2):146–59.
[10] Briscoe BJ, Sinha SK. Scratch resistance and localised damage characteristics of polymer surfaces – a review. Mat- wiss u Werkstofftech 2003;34(10–11):989–1002.
[11] Atkins AG. Toughness and cutting: a new way to simultaneously determining ductile fracture toughness and strength. Engng Fract Mech 2005;72:849–60.
[12] Sedriks AJ, Mulhearn TO. Mechanics of cutting and rubbing in simulated abrasive processes. Wear 1963;6(6):457–66.
[13] Sedriks AJ, Mulhearn TO. The effect of work-hardening on the mechanics of cutting in simulated abrasive processes. Wear 1963;7(5):451–9.
[14] Bowden FP, Tabor D. The friction and lubrication of solids, part I. Oxford: Clarendon Press; 1954.
[15] Merchant ME. Mechanics of the metal cutting process. I. Orthogonal cutting and a type 2 chip. J Appl Phys 1945;16(5):267–75.
[16] Childs THC. The sliding of rigid cones over metals in high adhesion condition. Int J Mech Sci 1970;12(5):393–403.
[17] Golden JH, Hammant BL, Hazell EA. The effect of thermal pretreatment on the strength of polycarbonate. J Appl Polym Sci 1967;11(8):1571–9.
[18] Bauwens-Crowet C, Bauwens JC. Annealing of polycarbonate below the glass transition: quantitative interpretation of the effect on yield stress and differential scanning calorimetry measurements. Polymer 1982;3(11):1599–604.
[19] van Breemen LCA. Contact mechanics in glassy polymers. PhD thesis, Eindhoven University of Technology; 2009.
[20] Gauthier C, Schirrer R. Time and temperature dependence of the scratch properties of poly(methylmethacrylate) surfaces. J Mater Sci 2000;35(9):2121–30.
[21] Roetling JA. Yield stress behaviour of polymethylmethacrylate. Polymer 1965;6(6):311–7.
[22] Ree T, Eyring H. Theory of non-Newtonian flow. I. Solid plastic system. J Appl Phys 1955;26(7):794–800.
[23] Bauwens-Crowet C, Bauwens JC, Homès G. Tensile yield-stress behavior of glassy polymers. J Polym Sci Pol Phys 1969;7(4):735–42.
[24] Kobayashi A. Machining of plastics. New York: McGraw-Hill; 1967.
[25] Callister Jr WD. Materials science and engineering: an introduction. 4th ed. John Wiley and Sons; 1996.
[26] Mandell JF, Darwish AY, McGarry FJ. Effects of processing conditions and aging on the fracture toughness of rigid PVC pipe materials. J Vinyl Technol 1982;4(3):95–100.
[27] Moore DR, Prediger R, Stephenson D. Relevance and application of fracture toughness measurements for uPVC. Plast Rub Proc Appl 1985;5(4):335–41.
[28] Wyeth DJ. An investigation into the mechanics of cutting using data from orthogonally cutting Nylon 66. Int J Mach Tool Manu 2008;48(7–8):896–904.